Supplementary Information

Designing Small Organic Molecular NIR-II Fluorophores by Ring Strain Modulation

Xingyu Wang, Tuanwei Li*, Xiaohu Yang, Xingyu Yang, Zhiwei Ma, Xiangyu, Wu, Yejun Zhang, Guangcun Chen, Jiang Jiang, and Chunyan Li*

X. Wang, Dr. T. Li,* Dr. X. Yang, X. Yang, Dr. Z. Ma, Dr. X. Wu, Dr. Y. Zhang, Prof. G. Chen, Prof. J. Jiang, and Prof. C. Li*

CAS Key Laboratory of Nano-Bio Interface, Division of Nanobiomedicine and *i*-Lab, Suzhou Institute of Nano-Tech and Nano-Bionics,

Chinese Academy of Sciences

Suzhou 215123, (China)

Email: cyli2012@sinano.ac.cn; twli2020@sinano.ac.cn

Reagents and apparatus

All chemical reagents were purchased from Aladdin Corporation (China) and Sinopharm Chemical Reagent Co., Ltd. (China), and were used as received. Experimental water was ultrapure water prepared by a Milli-Q synthesis system (18.2 M, Millipore). The ^{1}H-NMR and ^{13}C-NMR spectra were acquired by a Bruker AM 400 spectrometer. High-resolution electrospray ionization mass spectra (HR-ESI-MS) were recorded on a Bruker autoflex maX mass spectrometer. Liquid chromatography-mass spectrometry (LC−MS) analysis was measured by Q Exactive Plus (Thermo Fisher Scientific). The UV-Vis-NIR absorption spectra were recorded by a Perkin-Elmer Lambda 25 UV-Vis spectrometer. Fluorescence spectra were acquired from Applied Nano Fluorescence spectrometer (USA) and F-4600 FL spectrophotometer.

Synthetic procedures and characterization

Synthesis of compound 1. Compound 1 was synthesized according to our previous procedures.[1]

Synthesis of compound 2. Cyclohexanone (32.0 mmol, 2.0 eq.) and 2-(4-(Diethylamino)-2-hydroxybenzoyl) benzoic acid (5.0 g, 16.0 mmol, 1.0 eq.) were added into the H_2SO_4 (20 mL), and the reaction mixture was kept stirring at 0 °C for 30 min. Then the reaction temperature was increased to 90

°C and reacted for another 2.0 h. After being cooled to room temperature, the mixture was poured into ice, and then 70% perchloric acid (5 mL) was added subsequently. The red precipitate was then filtered, washed and dried under vacuum to obtain compound 2 (7.1 g, 94% yield). ^{1}H NMR (400 MHz, Chloroform-d) δ 8.27 (dd, J = 7.9, 1.2 Hz, 1H), 7.76 (td, J = 7.6, 1.3 Hz, 1H), 7.67 (td, J = 7.7, 1.3 Hz, 1H), 7.20 (d, J = 7.1 Hz, 1H), 7.11-7.01 (m, 2H), 6.87 (d, J = 2.2 Hz, 1H), 3.62 (q, J = 7.2 Hz, 4H), 3.15-3.01 (m, 2H), 2.26 (dtd, J = 22.8, 16.4, 6.2 Hz, 2H), 1.96 (q, J = 9.1, 6.5 Hz, 2H), 1.78 (d, J = 10.2 Hz, 2H), 1.32 (t, J = 7.1 Hz, 6H). ^{13}C NMR (101 MHz, DMSO-d6) δ 166.84, 159.19, 155.73, 134.66, 133.65, 131.28, 130.80, 130.32, 129.87, 129.07, 120.94, 118.97, 117.04, 116.72, 95.68, 45.97, 29.29, 25.18, 23.17, 22.99, 21.41, 21.12. HR-MS m/z calcd for $C_{24}H_{26}NO_3^+$, $[M\text{-}ClO_4]^+$: 376.1907, found: 376.1900.

Synthesis of compound 3. Cycloheptanone (32.0 mmol, 2.0 eq.) and 2-(4-(Diethylamino)-2-hydroxybenzoyl) benzoic acid (5.0 g, 16.0 mmol, 1.0 eq.) was added into the H_2SO_4 (20 mL), and the reaction mixture was kept stirring at 0 °C for 30 min. Then the reaction temperature was increased to 90 °C and reacted for another 2.0 h. After being cooled to room temperature, the mixture was poured into ice, and then 70% perchloric acid (5 mL) was added subsequently. The red precipitate was then filtered, washed and dried under vacuum to obtain compound 3 (7.2 g, 92% yield). ^{1}H NMR (400 MHz, Chloroform-d) δ 8.27 (dd, J = 7.9, 1.3 Hz, 1H), 7.75 (td, J = 7.5, 1.4 Hz, 1H), 7.67 (td, J = 7.7, 1.3 Hz, 1H), 7.14 (dd, J = 7.6, 1.3 Hz, 1H), 7.07-6.98 (m, 2H), 6.86 (d, J = 2.0 Hz, 1H), 3.58 (q, J = 7.2 Hz, 4H), 3.31-3.17 (m, 2H), 2.44 (t, J = 5.6 Hz, 2H), 1.86 (s, 4H), 1.61 – 1.45 (m, 2H), 1.28 (t, J = 7.1 Hz, 6H). ^{13}C NMR (101 MHz, CDCl3) δ 175.71, 166.38, 165.09, 158.98, 155.33, 134.90, 133.42, 131.85, 130.46, 130.41, 129.12, 128.60, 127.14, 118.20, 117.16, 116.69, 95.42, 46.18, 36.16, 31.38, 28.60, 25.73, 24.75. HR-MS m/z calcd for $C_{25}H_{28}NO_3^+$, $[M\text{-}ClO_4]^+$: 390.2064, found: 390.2059.

Synthesis of Rh5. Compound 1 (0.92 g, 2.0 mmol, 2.0 eq.) and malondialdehyde bis(phenylimine) monohydrochloride (0.26 g, 1.0 mmol, 1.0 eq.) were dissolved in 20 mL of acetic anhydride, and then the mixture was refluxed in nitrogen at 110 °C for 1.5 h. When the temperature was cooled to 45 °C, 10 mL pyridine was added dropwise. The mixture was stirred at 45 °C for another 6 h before evaporating the solvent under reduced pressure. The crude product was purified using silica gel column chromatography with a gradient elution (DCM: methanol = 10:1) to get Rh5 as a black powder. Then the product was further purified by high-performance liquid chromatography (HPLC) to obtain Rh5 (0.25 g, 29% yield). ^{1}H NMR (400 MHz, DMSO-d6) δ 12.98 (s, 2H), 8.07 (dd, J = 7.8, 1.5 Hz, 2H), 7.79 – 7.70 (m, 2H), 7.68 – 7.55 (m, 4H), 7.32 (d, J = 7.5 Hz, 2H), 6.81 – 6.65 (m, 6H), 6.30 (t, J = 13.3 Hz, 1H), 3.47 (q, J = 7.2 Hz, 8H), 2.78 (d, J = 6.6 Hz, 4H), 2.60 (dt, J = 13.5, 6.4 Hz, 2H), 2.45 (m, 2H), 1.14 (t, J = 7.1 Hz, 12H). ^{13}C NMR (101 MHz, DMSO-d6) δ 167.45, 164.20, 155.92, 151.23, 145.48, 138.63, 134.99, 133.12, 131.63, 131.11, 131.08, 130.06, 129.82, 127.34, 124.27, 122.27, 114.01, 112.26, 97.35, 44.91, 25.26, 24.63, 12.87. HR-MS m/z calcd for $C_{49}H_{47}N_2O_6^+$, $[M\text{-}ClO_4]^+$: 759.3429, found: 759.3409.

Synthesis of Rh6. Compound 2 (0.95 g, 2.0 mmol, 2.0 eq.) and malondialdehyde bis(phenylimine)

monohydrochloride (0.26 g, 1.0 mmol, 1.0 eq.) were dissolved in 20 mL of acetic anhydride, and then the mixture was refluxed in nitrogen at 100 °C for 1.5 h. When the temperature was cooled to room temperature, sodium acetate (0.25 g, 3 mmol, 3.0 eq.) was added. The mixture was stirred at 25 °C overnight before evaporating the solvent under reduced pressure. The crude product was purified using silica gel column chromatography with a gradient elution (DCM : methanol = 10:1) to get Rh6 as a black powder. Then the product was further purified by HPLC to obtain Rh6 (0.29 g, 33% yield). ^{1}H NMR (400 MHz, DMSO-d6) δ 12.94 (s, 2H), 8.16 – 8.05 (m, 4H), 7.79 – 7.73 (m, 2H), 7.65 (t, J = 7.7 Hz, 2H), 7.30 (d, J = 7.6 Hz, 2H), 6.89 (d, J = 2.4 Hz, 2H), 6.75 (dd, J = 9.2, 2.5 Hz, 2H), 6.68 (d, J = 13.3 Hz, 1H), 6.56 (d, J = 9.1 Hz, 2H), 3.50 (q, J = 7.1 Hz, 8H), 2.69 – 2.59 (m, 4H), 2.26 – 2.12 (m, 4H), 1.68 (dt, J = 30.2, 7.5 Hz, 4H), 1.17 (t, J = 7.0 Hz, 12H). ^{13}C NMR (101 MHz, DMSO-d6) δ 167.23, 159.48, 155.85, 151.88, 149.48, 142.90, 135.75, 133.16, 131.07, 130.98, 130.07, 129.67, 127.93, 121.52, 120.84, 117.96, 113.84, 112.40, 96.45, 44.86, 26.82, 24.86, 20.79, 12.99. HR-MS m/z calcd for $C_{51}H_{51}N_2O_6^+$, $[M\text{-}ClO_4]^+$: 787.3742, found: 787.3715.

Synthesis of Rh7. Compound 3 (0.98 g, 2 mmol, 2.0 eq.) and malondialdehyde bis(phenylimine) monohydrochloride (0.26 g, 1 mmol, 1.0 eq.) were dissolved in 20 mL of acetic anhydride, and then the mixture was refluxed in nitrogen at 110 °C for 2 h. When the temperature was cooled to 80 °C, sodium acetate (0.82 g, 10 mmol, 10 eq.) was added. The mixture was stirred at 80 °C for another 3 h before evaporating the solvent under reduced pressure. The crude product was purified using silica gel column chromatography with a gradient elution (DCM : methanol = 10:1) to get Rh7 as a black powder. Then the product was further purified by HPLC to obtain Rh7 (0.09 g, 10% yield). ^{1}H NMR (400 MHz, DMSO-d6) δ 8.17 – 7.97 (m, 4H), 7.76 (td, J = 7.6, 1.5 Hz, 2H), 7.65 (t, J = 7.6 Hz, 2H), 7.30 (d, J = 7.5 Hz, 2H), 6.90 (s, 2H), 6.80 – 6.68 (m, 2H), 6.51 (ddd, J = 12.3, 6.8, 3.5 Hz, 3H), 3.65 – 3.36 (m, 8H), 2.78 (dd, J = 18.3, 11.0 Hz, 4H), 2.40 – 2.21 (m, 4H), 1.78 (dd, J = 23.2, 12.5 Hz, 4H), 1.67 – 1.52 (m, 4H), 1.15 (t, J = 7.0 Hz, 12H). ^{13}C NMR (101 MHz, DMSO-d6) δ 167.24, 163.13, 158.83, 158.47, 155.86, 152.23, 151.86, 145.94, 136.37, 133.13, 131.16, 131.03, 130.26, 129.66, 128.01, 123.99, 123.19, 119.85, 117.44, 114.60, 114.01, 112.48, 96.25, 44.84, 27.05, 25.15, 24.90, 24.28, 12.96. HR-MS m/z calcd for $C_{53}H_{55}N_2O_6^+$, $[M\text{-}ClO_4]^+$: 815.4055, found: 815.4023.

Theoretical calculations. The theoretical calculations were employed using the Gaussian 16W software package to optimize the geometries of these probes and understand their structural and electronic properties. The density functional theory (DFT) and time-department DFT (TD-DFT) calculations were adopted at M062X/6-31G (d,p) basis sets.[2] The planarity of probes and the local electron attachment energy was quantified and graphically investigated using Multiwfn program according to the method reported by Tian Lu.[3,4]

Calculation of molar extinction coefficient (*ε*) and quantum yield (QY). The molar extinction coefficient was calculated according to the Lambert-Beer law as below:

$$A = \varepsilon bc$$

where A is the absorbance at the maximum absorption wavelength, ε is the molar extinction coefficient, b is the absorption thickness of optical path (1 cm), c is the concentration of the solution.

The fluorescence quantum yield of the probes was calculated according to the following calculations with IR-26 (Φ=0.05% in 1,2-dichloroethane) as reference:

$$\emptyset_s = \emptyset_r \times \frac{n_s^2}{n_r^2}\left(\frac{k_s}{k_r}\right)$$

Where $\emptyset_s$ and $\emptyset_r$ are the QY of the samples and IR-26, n_s and n_r are the refractive indices of the solvents, k_s and k_r are the slopes of the samples and IR-26. The QY of IR-26 was determined to be 0.05% in 1,2-dichloroethane.

Determination of pK_{cycl}.

The final concentration of probes was set at 10 μM in a 2 mL PBS buffer solution containing 50% ACN. The pH of the test solution was adjusted by adding HCl (100 mM) or NaOH (100 mM). The absorption and emission spectra were recorded in different buffers (pH 1.00 to pH 13.0). The pK_{cycl} is defined as the pH at which the emission of the probe decreases to half the maximum emission due to the spirocyclization.

Fluorescence response towards pH. Rh5 solutions (10 μM) were incubated in PBS/ACN (v/v, 1/1) buffer solution and PBS/FBS (v/v, 9/1) buffer solution with different pH values for 2 h, respectively. Then the absorbance and NIR fluorescence spectra were measured to evaluated the response.

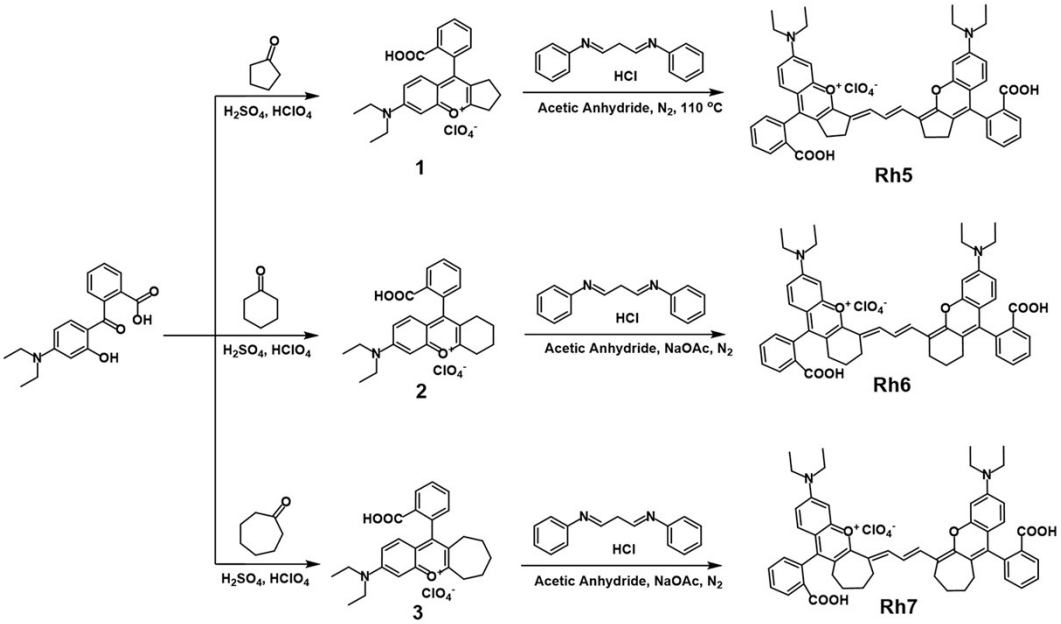

Scheme S1. Scheme for the design and synthesis of Rh probes.

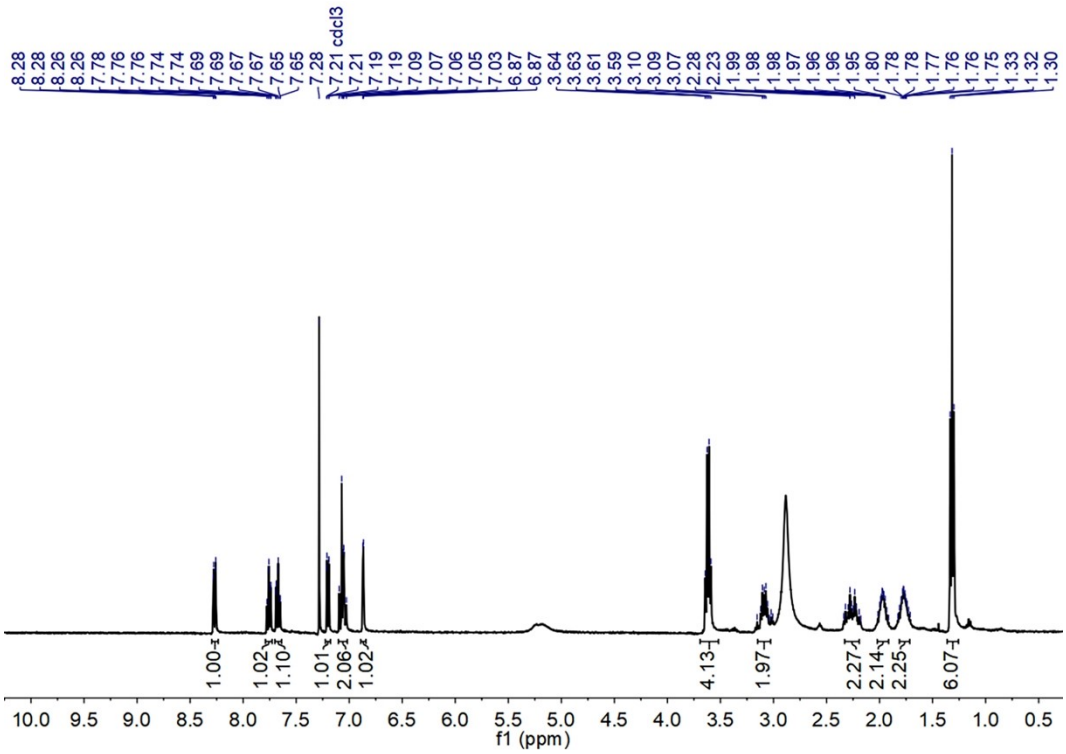

Figure S1. ^{1}H NMR of Compound 2 in $CDCl_3$.

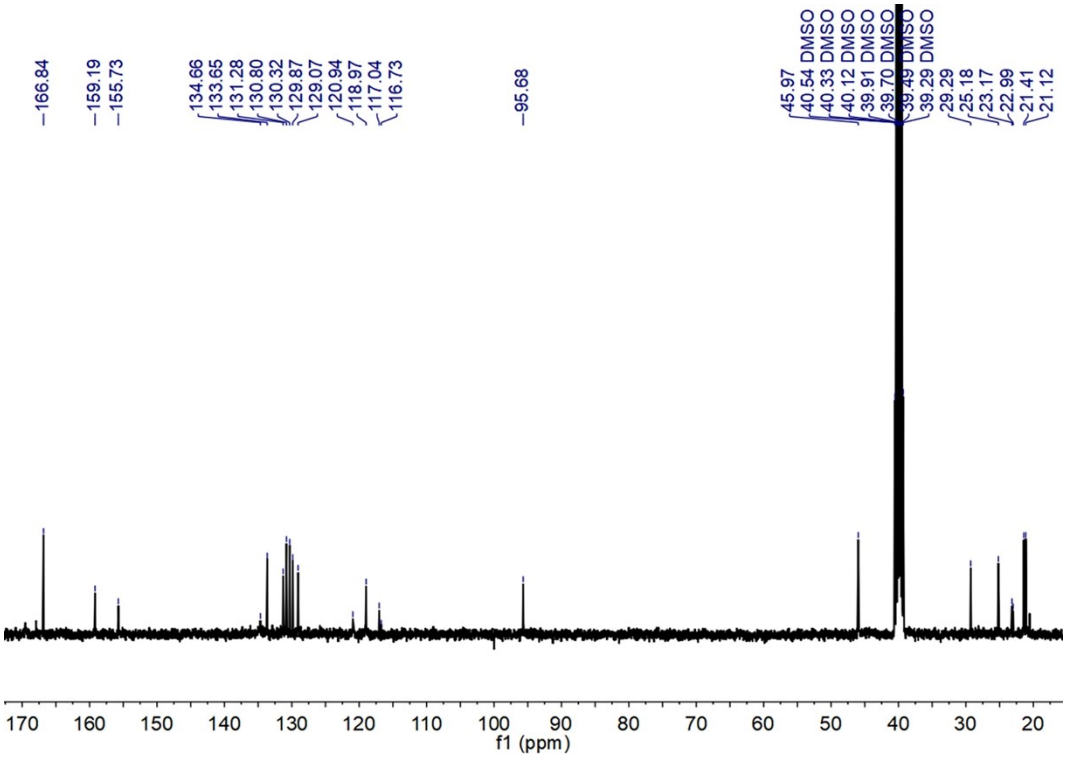

Figure S2. ^{13}C NMR of Compound 2 in DMSO-d6.

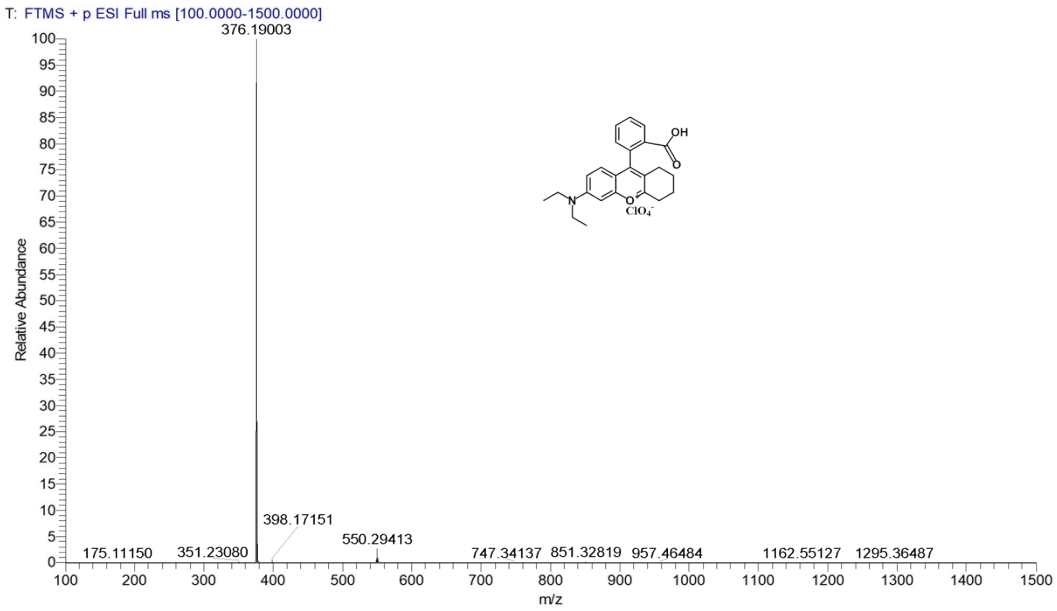

Figure S3. HR-MS of Compound 2.

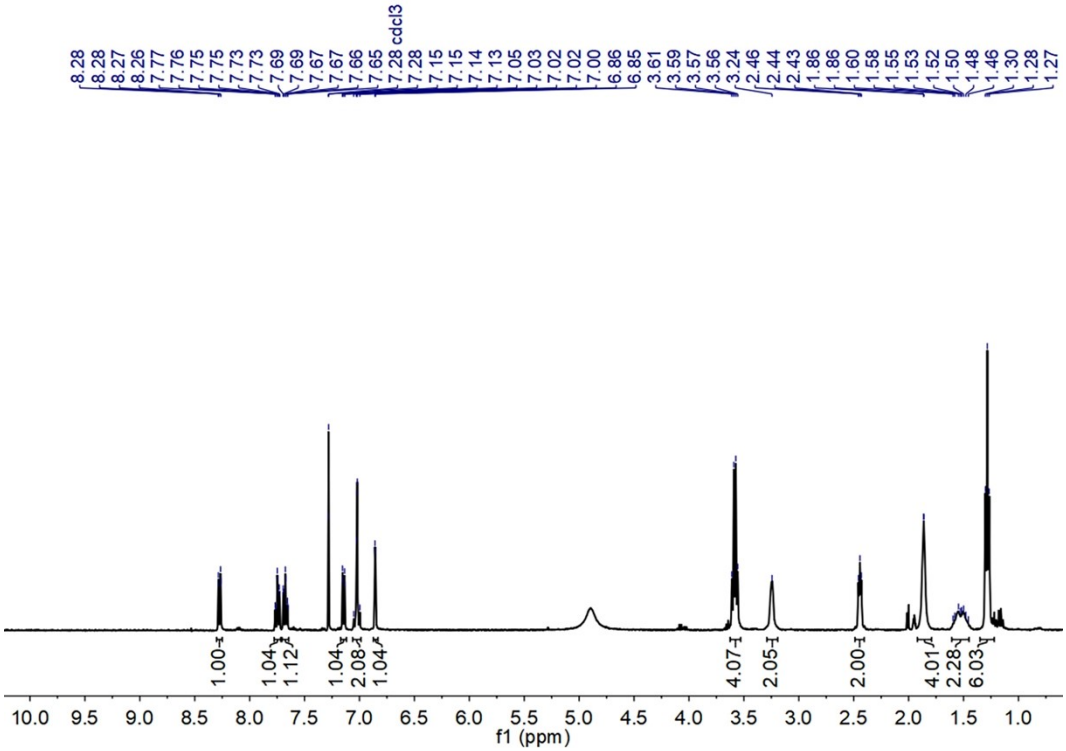

Figure S4. ^{1}H NMR of Compound 3 in $CDCl_3$.

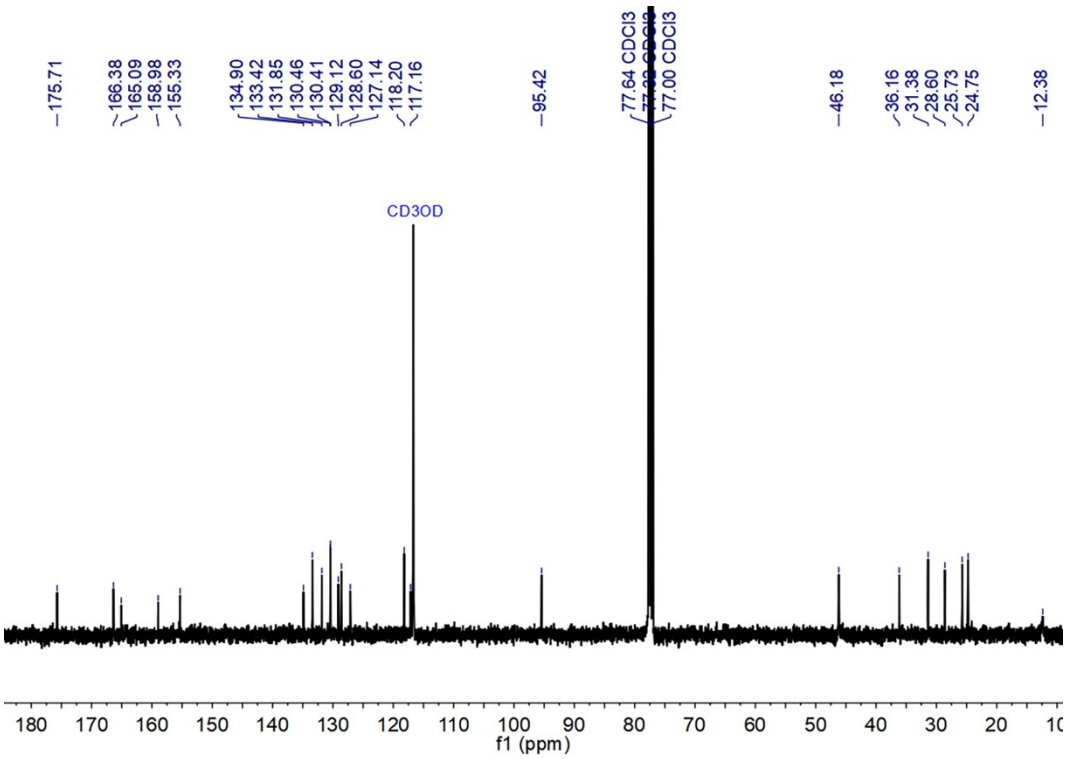

Figure S5. ^{13}C NMR of Compound 3 in $CDCl_3$ and CD_3OD.

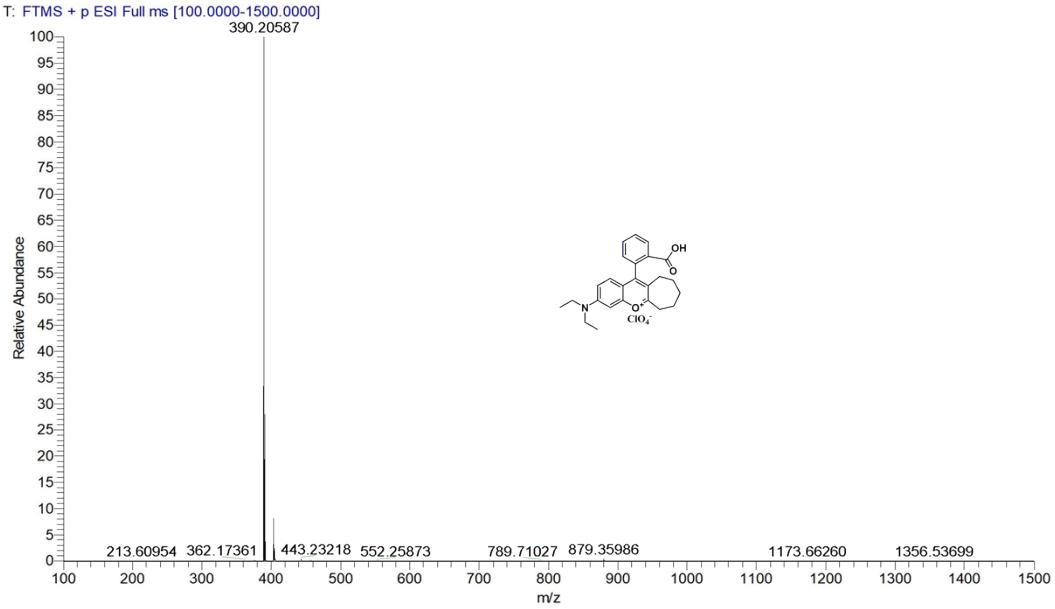

Figure S6. HR-MS of Compound 3.

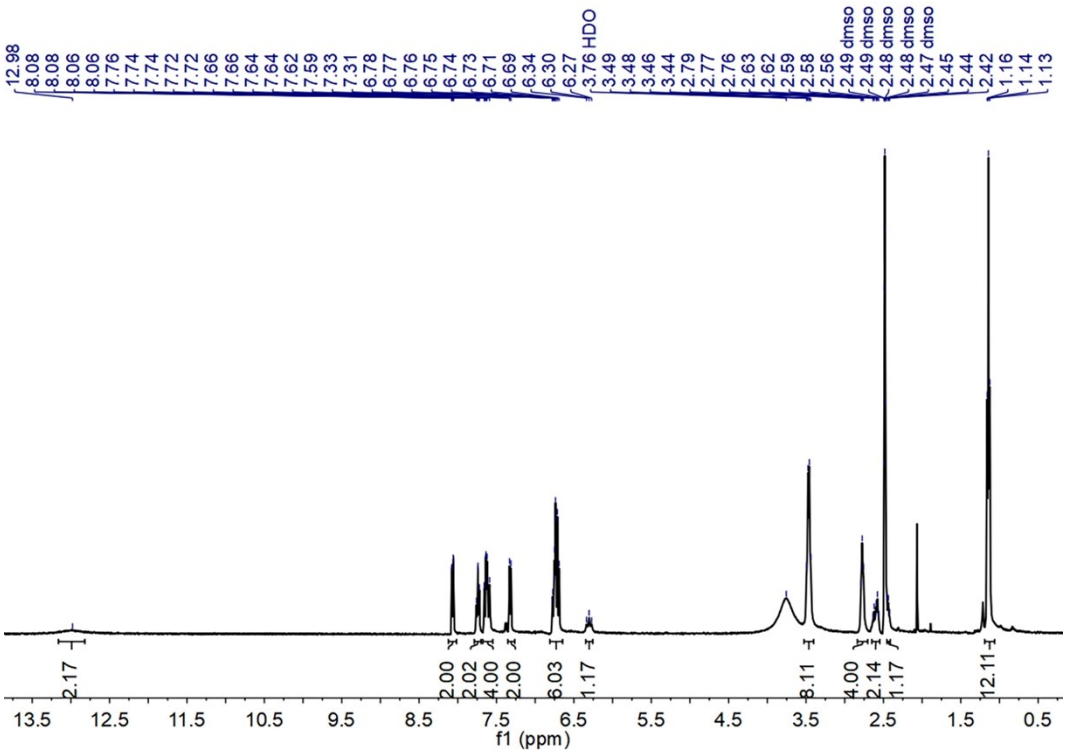

Figure S7. ^{1}H NMR of Rh5 in DMSO-d6.

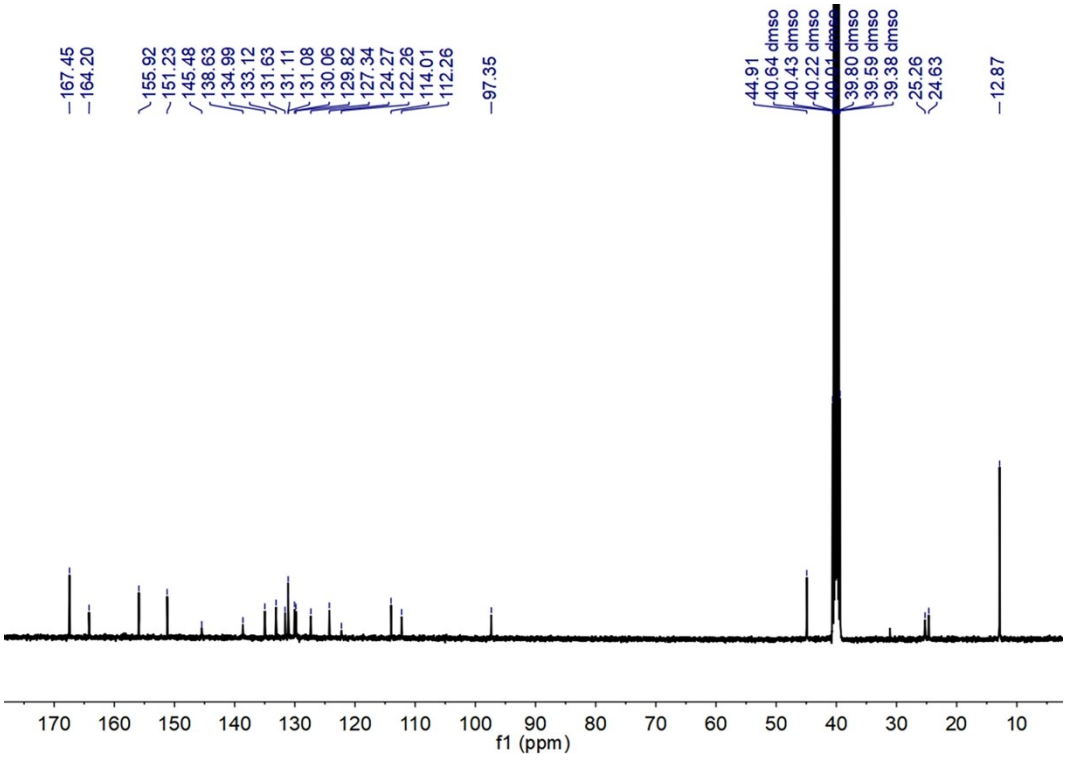

Figure S8. ^{13}C NMR of Rh5 in DMSO-d6.

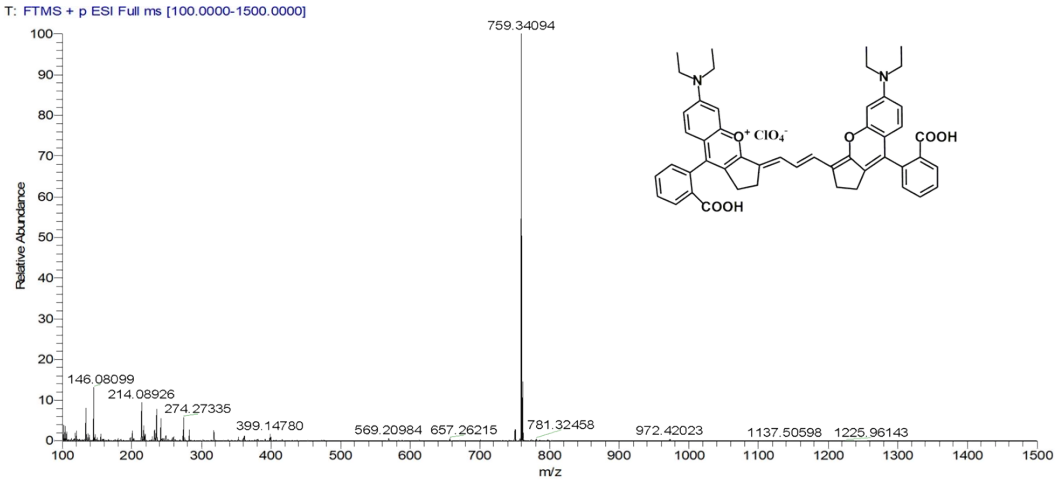

Figure S9. HR MS of Rh5.

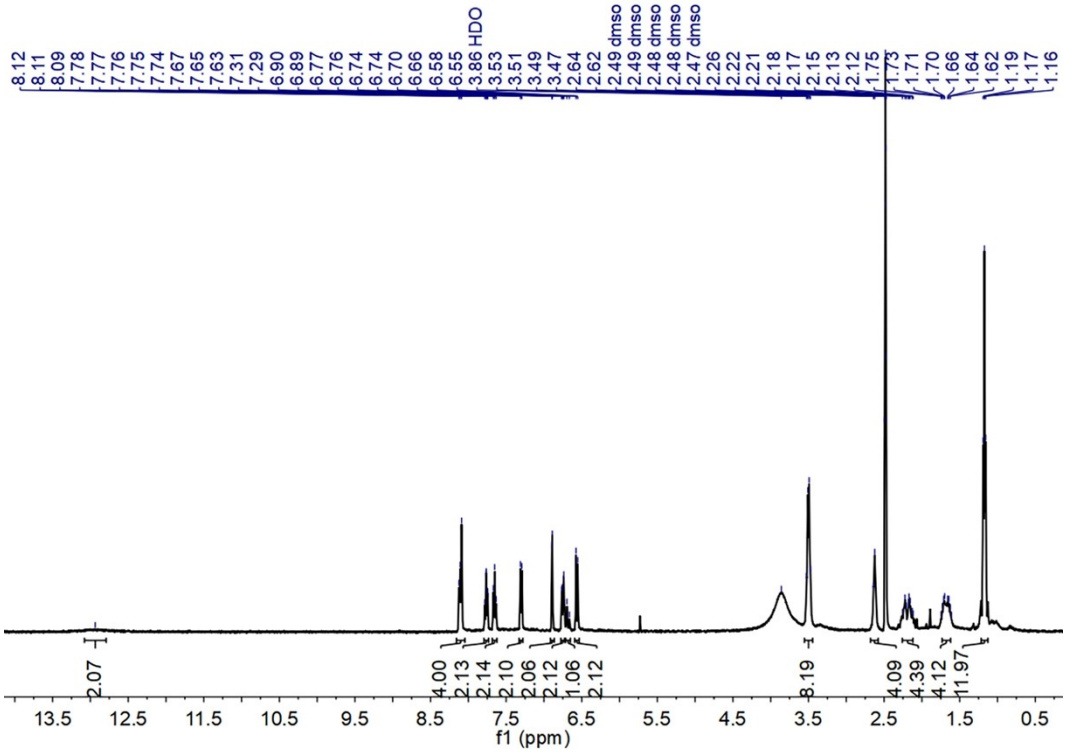

Figure S10. [1]H NMR of Rh6 in DMSO-d6.

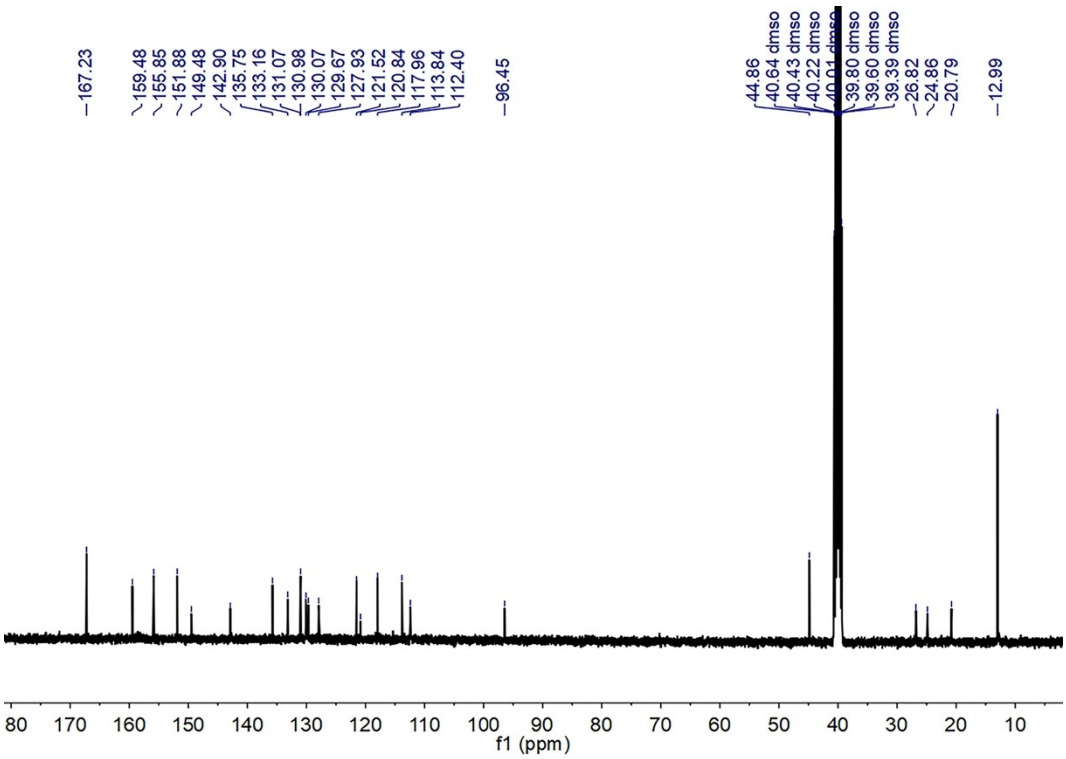

Figure S11. ^{13}C NMR of Rh6 in DMSO-d6.

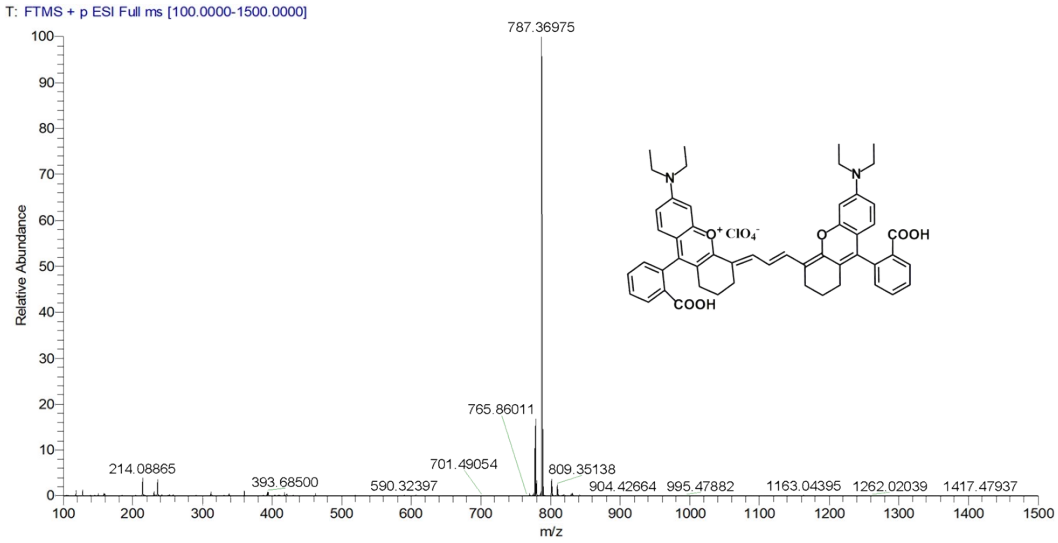

Figure S12. HR MS of Rh6.

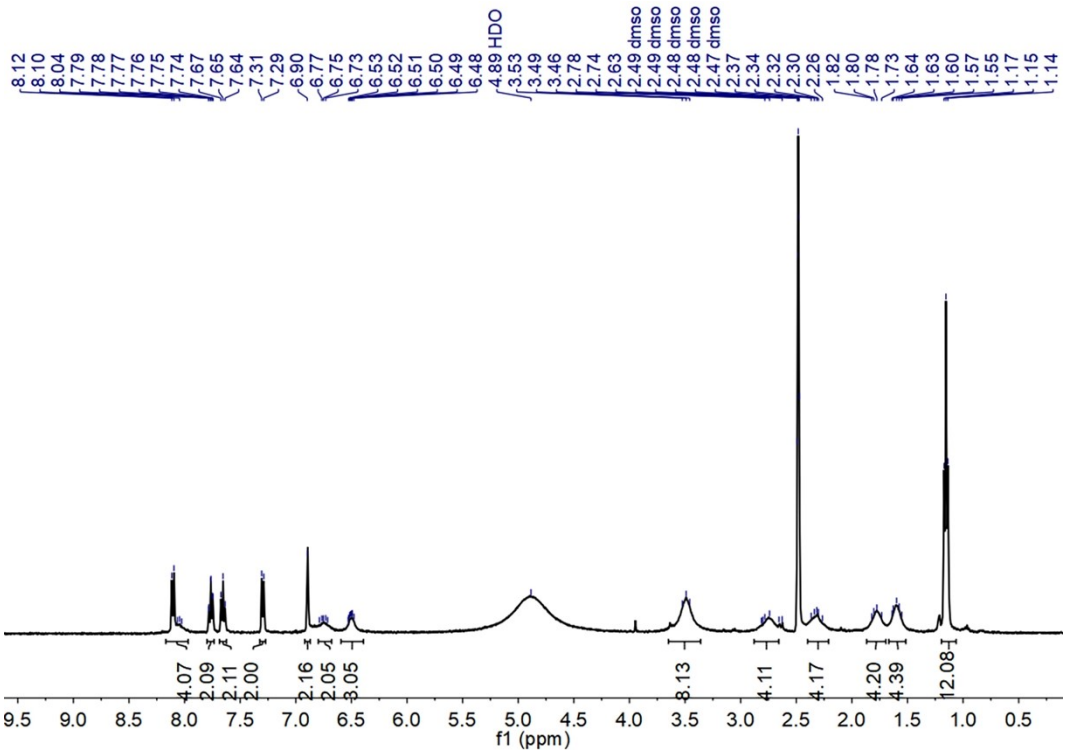

Figure S13. ^{1}H NMR of Rh7 in DMSO-d6.

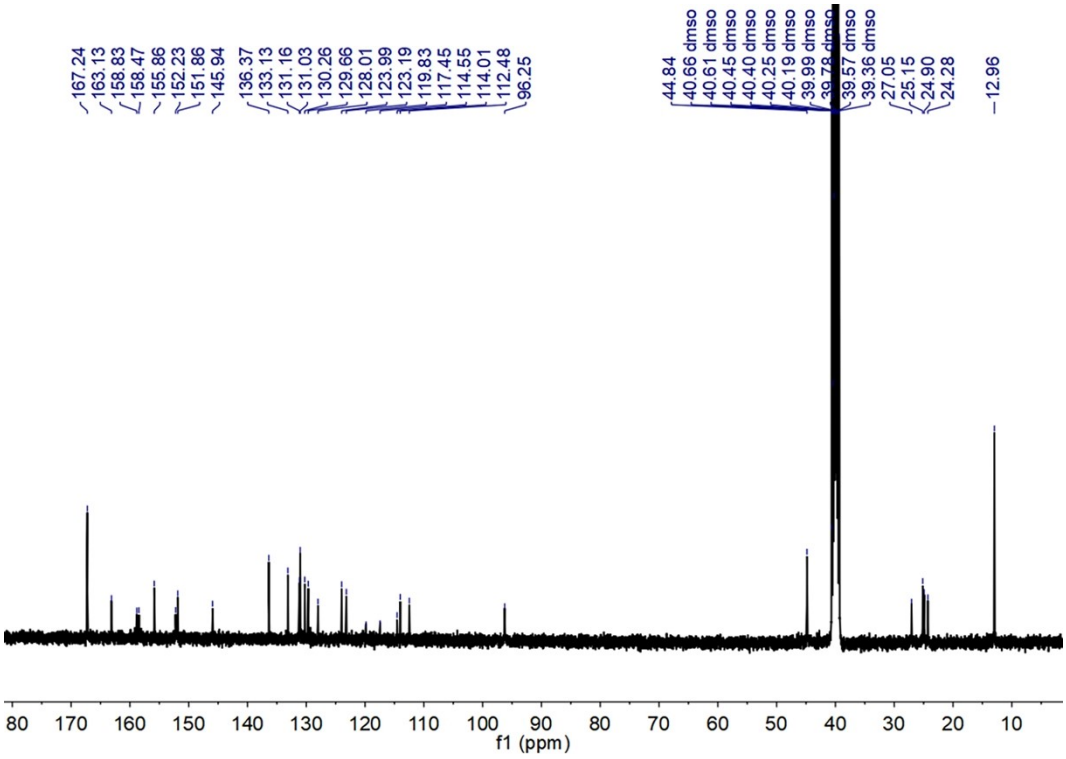

Figure S14. ^{13}C NMR of Rh7 in DMSO-d6.

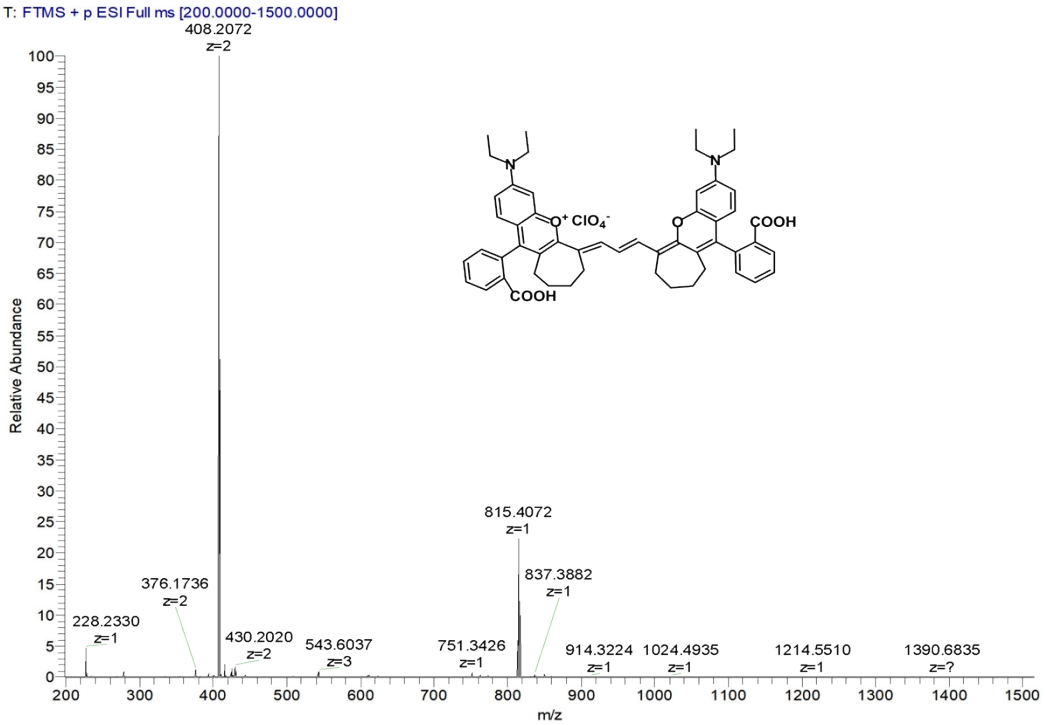

Figure S15. HR MS of Rh7.

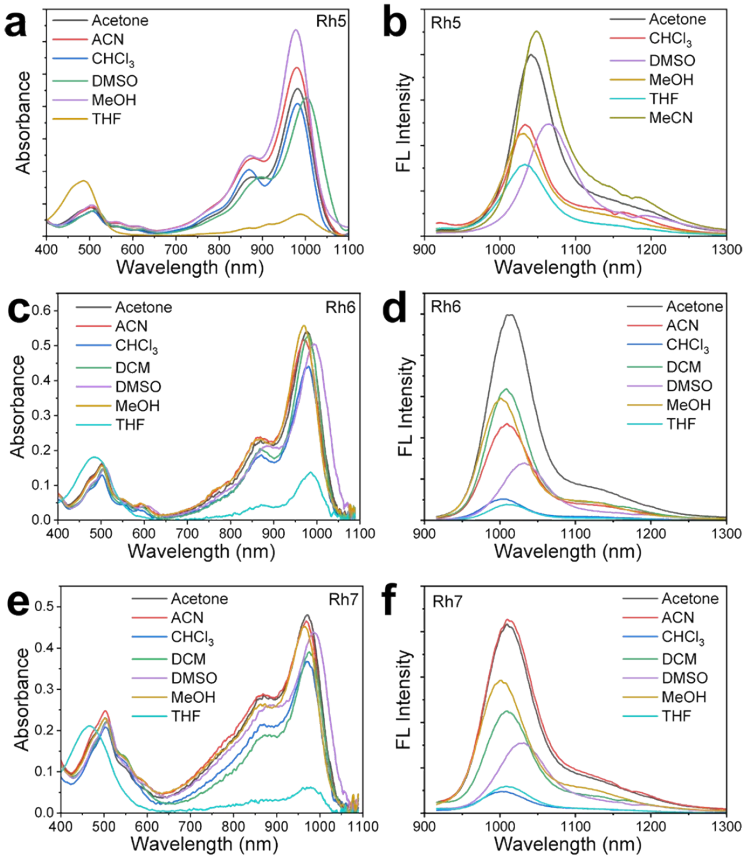

Figure S16. The absorption (a) and fluorescence emission spectra (b) of Rh5 in different solvents. The absorption (c) and fluorescence emission spectra (d) of Rh6 in different solvents. The absorption (e) and fluorescence emission spectra (f) of Rh7 in different solvents.

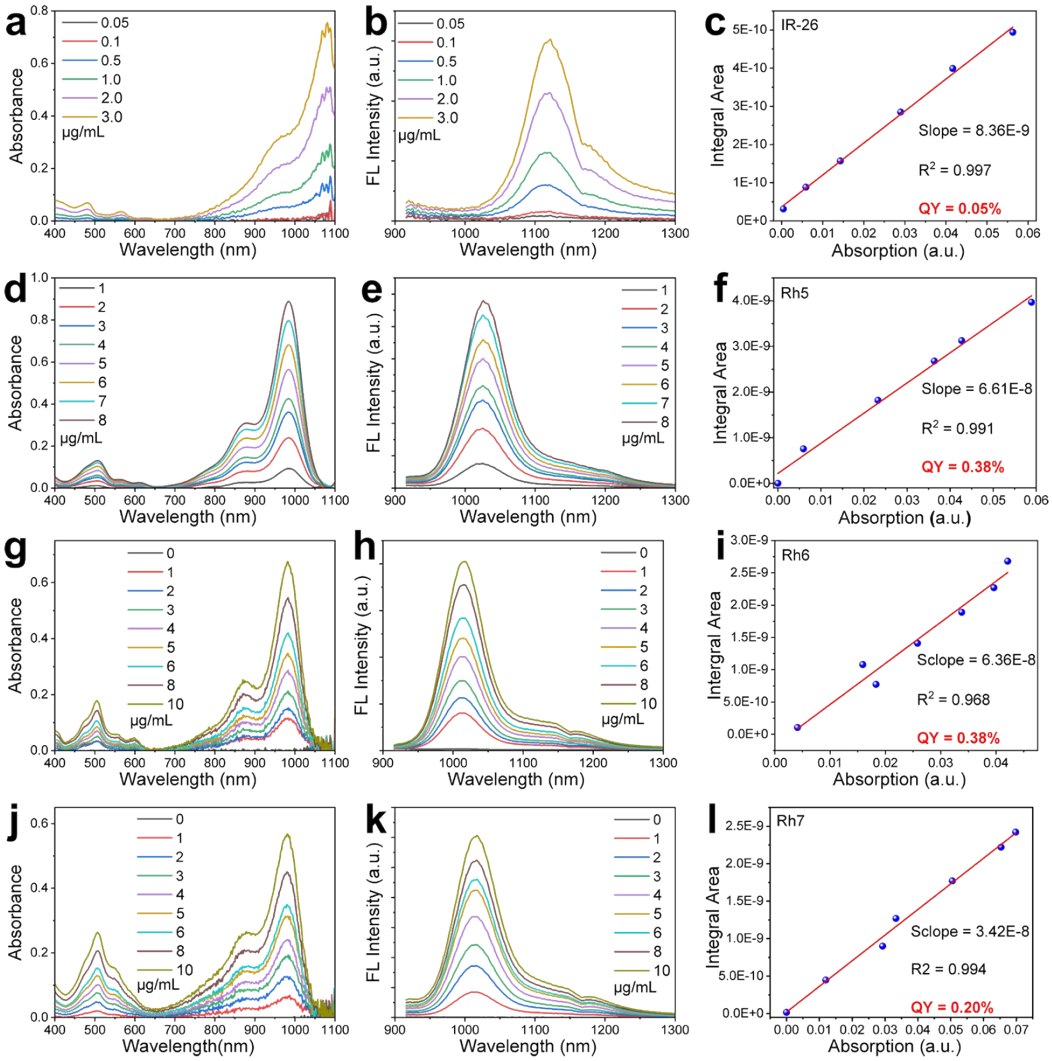

Figure S17. Relative fluorescence quantum yield of Rh5 probes. The absorption (a), fluorescence emission spectra (b) and plot of fluorescence intensity of IR 26 (c) at different absorption. The fluorescence quantum yield of IR 26 was 0.05% in DCE. The absorption (d), fluorescence emission spectra (e) and plot of fluorescence intensity of Rh5 (f) at different absorption in acetone. The absorption (g), fluorescence emission spectra (h) and plot of fluorescence intensity of Rh6 (i) at different absorption in DCE. The absorption (j), fluorescence emission spectra (k) and plot of fluorescence intensity of Rh7 (l) at different absorption in DCE.

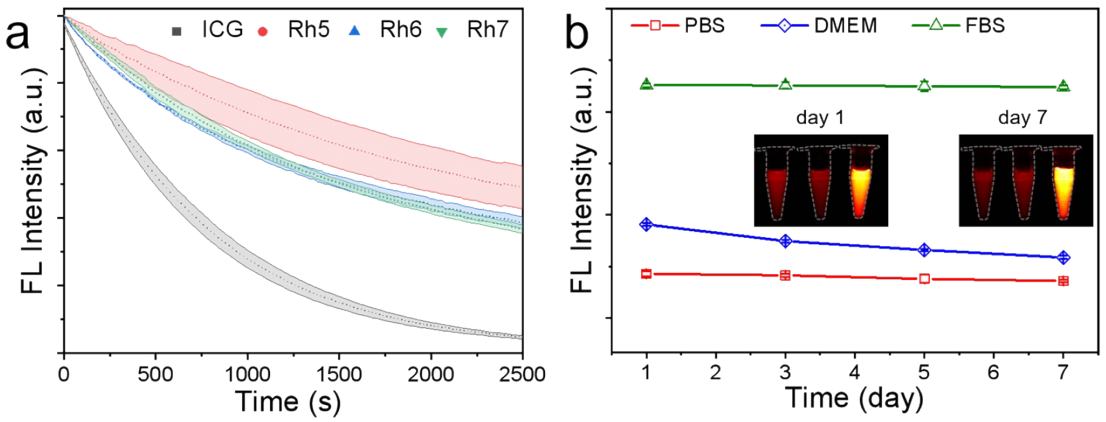

Figure S18. (a) Photostability of Rh probes and ICG in PBS with 50% FBS under continuous 808 nm exposure at a power density of 30 $mWcm^{-2}$, respectively. n=3. (b) The fluorescence stability of Rh5 in different biological medium for 7 days. Error bar n=3.

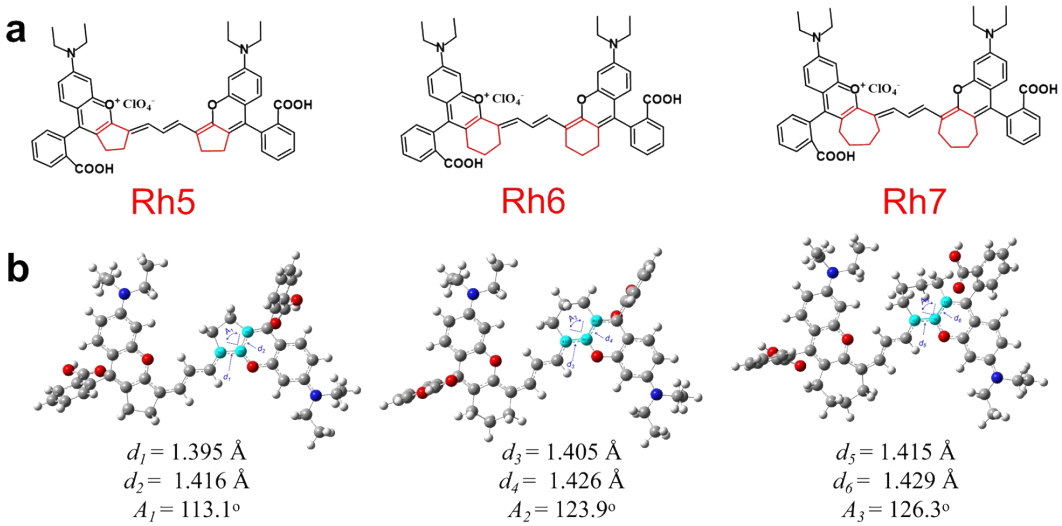

Figure S19. (a) Schematic chemical structures of Rh5, Rh6 and Rh7. (b) The bond length and bond angle for the pentatomic, hexatomic, and heptatomic ring structures.

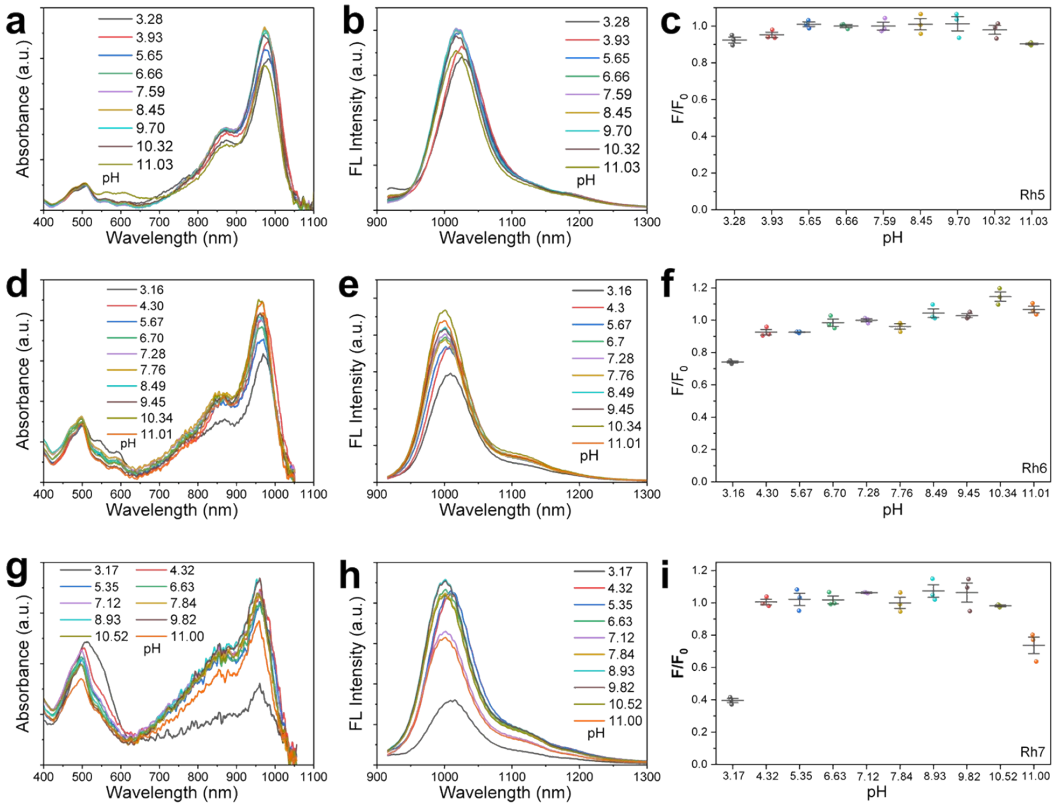

Figure S20. The optical properties of Rh probes at various pH values in PBS solution containing 50% ACN. The absorption (a), fluorescence emission spectra (b) and fluorescence intensity change ($F/F_{0,}$ c) of Rh5 at various pH values. The absorption (d), fluorescence emission spectra (e) and fluorescence intensity change ($F/F_{0,}$ f) of Rh6 at various pH values. The absorption (g), fluorescence emission spectra (h) and fluorescence intensity change ($F/F_{0,}$ i) of Rh7 at various pH values. Data are expressed as mean ± SD. Error bar: mean ± s.d. (n =3).

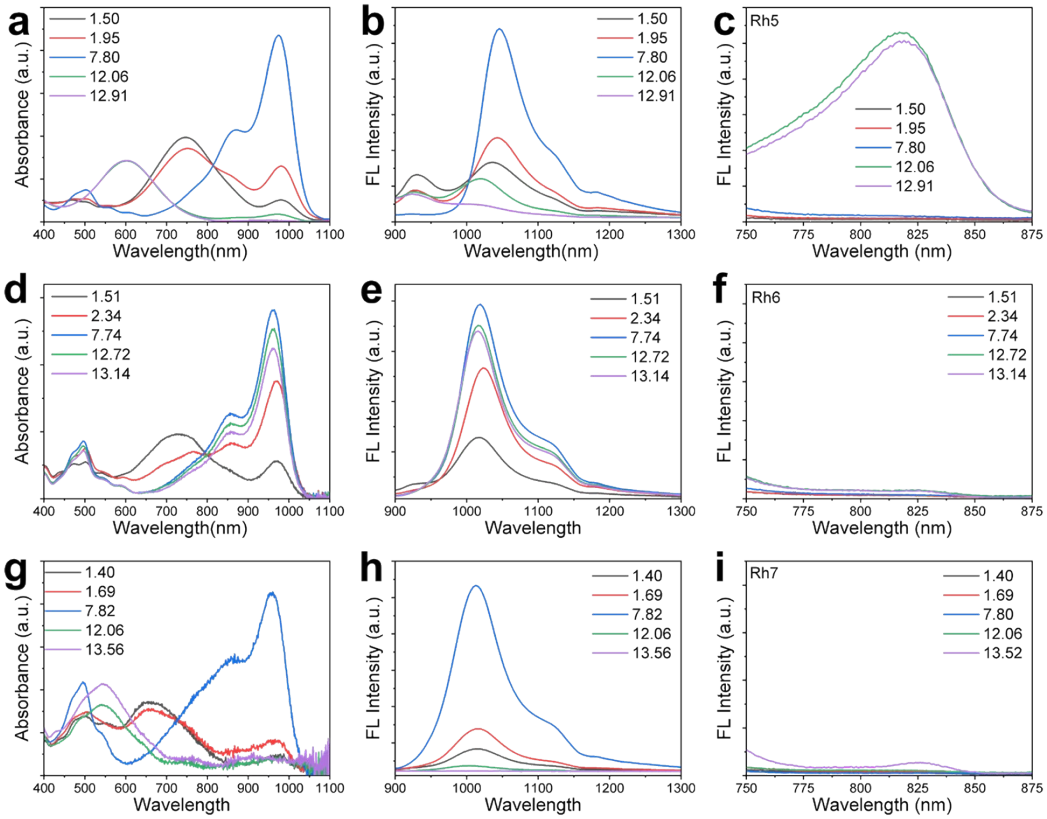

Figure S21. The optical properties of Rh probes at various pH values in PBS solution containing 50% ACN. The absorption (a), NIR-II fluorescence emission spectra (b) and NIR-I fluorescence emission spectra (c) of Rh5 at various pH values. The absorption (d), NIR-II fluorescence emission spectra (e) and NIR-I fluorescence emission spectra (f) of Rh6 at various pH values. The absorption (g), NIR-II fluorescence emission spectra (h) and NIR-I fluorescence emission spectra (i) of Rh7 at various pH values. (n =3).

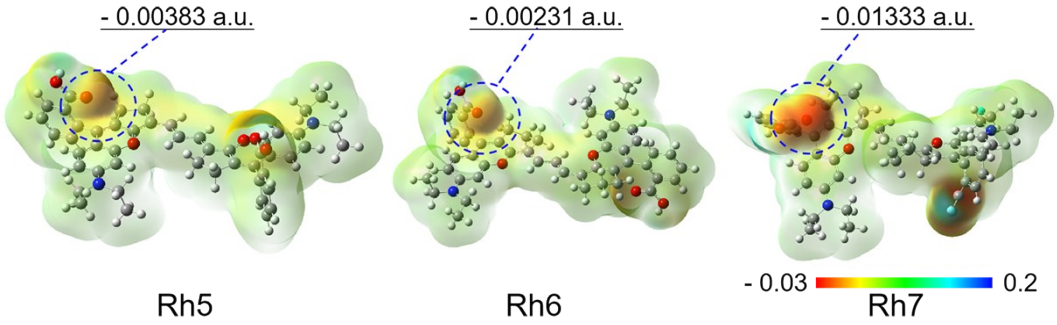

Figure S22. The ESP maps of Rh5, Rh6 and Rh7.

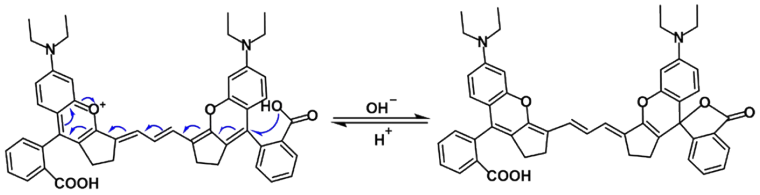

Figure S23. Proposed mechanism for pH recognition of Rh5.

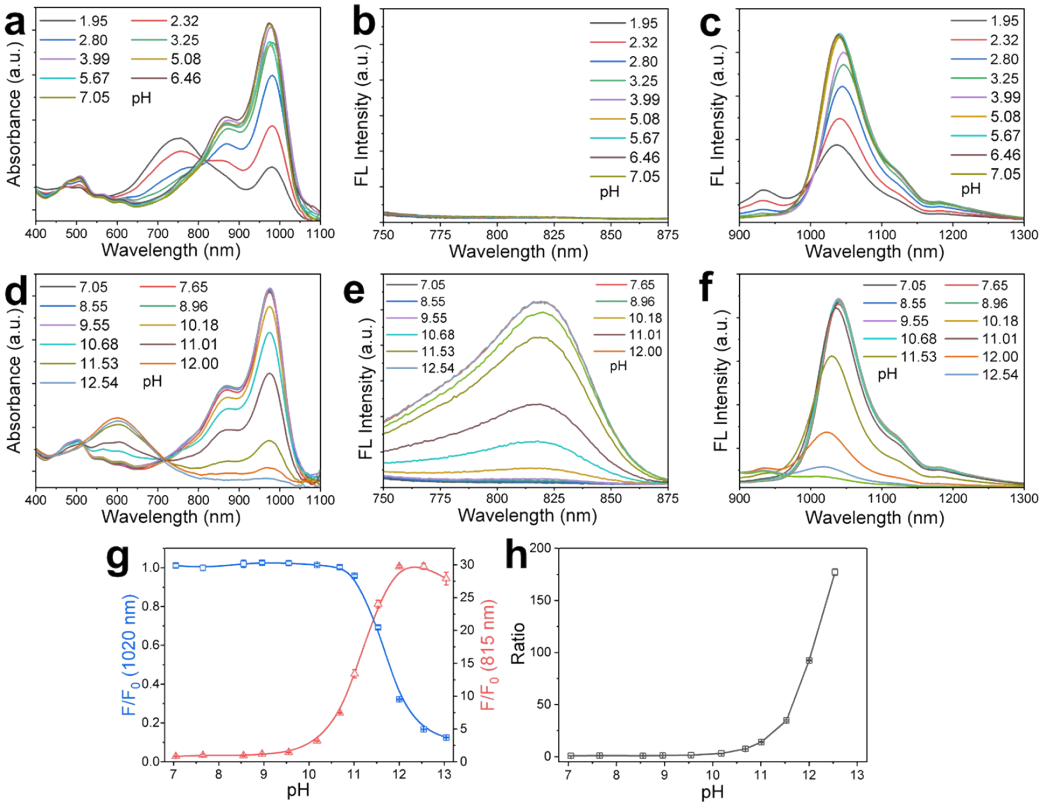

Figure S24. The optical properties of Rh probes at various pH values in PBS solution containing 50% ACN. The absorption (a, d), NIR-I fluorescence emission spectra (b, e) and NIR-II fluorescence emission spectra (c, f) of Rh5 in the acid environment. Plots of fluorescence intensities at 1020 and 815 nm (g) and ratio intensity (h) as a function of pH values in PBS/ACN (v/v, 1/1) buffer solution.

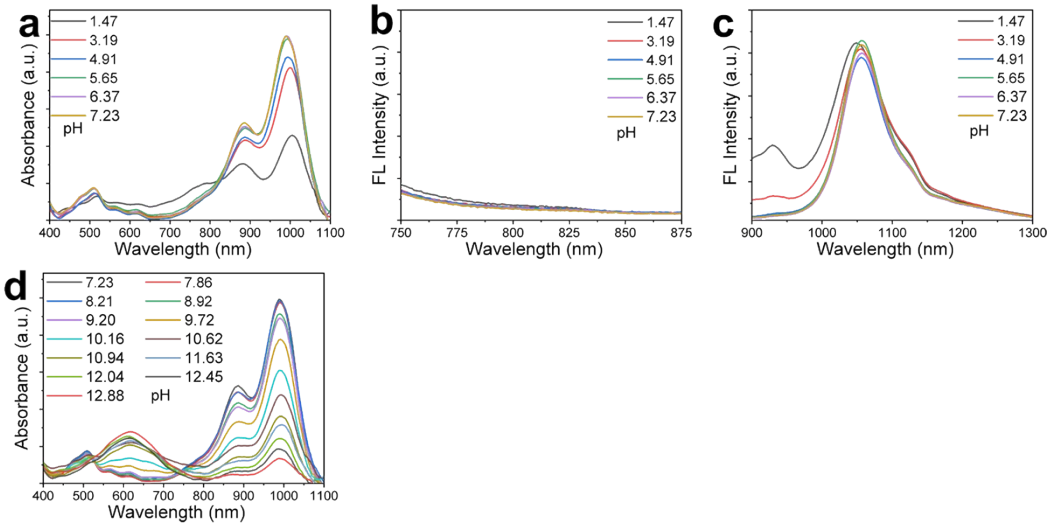

Figure S25. The optical properties of Rh probes at various pH values in PBS solution containing 10% FBS. The absorption (a), NIR-I fluorescence emission spectra (b) and NIR-II fluorescence emission spectra (c) of Rh5 in the acid environment. (d) The absorption in the alkaline environment of Rh5.

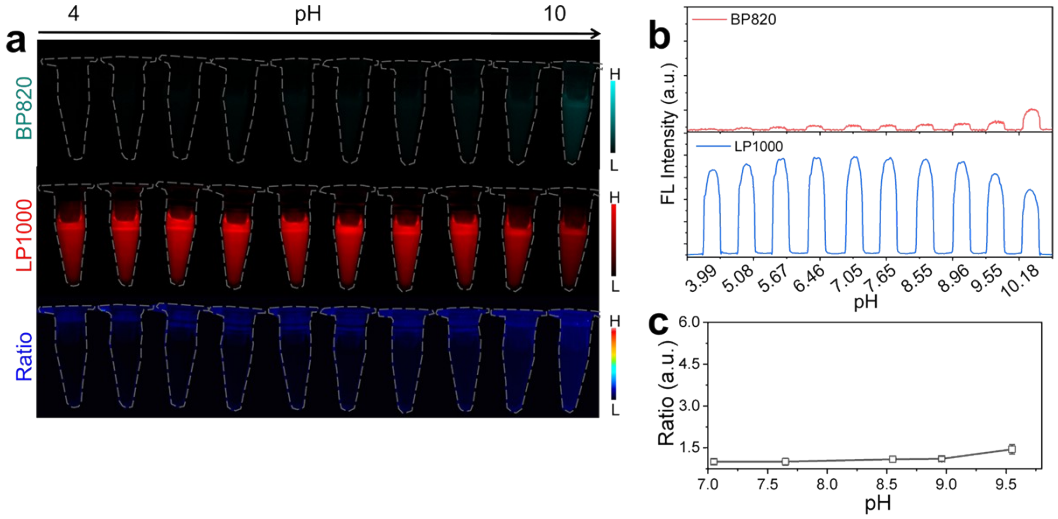

Figure S26. (a) Fluorescence and ratiometric fluorescence images of Rh5 (10 μM) incubated in PBS/ACN (v/v, 1/1) buffer solution with different pH values. (b) Quantification of fluorescence intensity in the BP820 and LP1000 channels in PBS/ACN (v/v, 1/1) buffer solution with different pH values. (c) Quantification of ratiometric signals of Rh5 as a function of the pH in PBS/ACN buffer solution.

References

[1] T. Li, K. Cao, X. Yang, Y. Liu, X. Wang, F. Wu, G. Chen, Q. Wang, *Biomaterials,* 2023, **293**, 121956.

[2] J. P. Perdew, K. Burke, M. Ernzerhof, *Phys. Rev. Lett.,* 1996, **77**, 3865-3868.

[3] T. Lu, *J. Mol. Model,* 2021, **27**, 263.

[4] T. Lu, Z. Liu, Q. Chen, *Chin. Phys. B* 2022, **31**, 126101.